Mathematical equivalence of non-local transport models and broadened deposition profiles

M. van Berkel[1], G. Vandersteen[2], H.J. Zwart[3,4], G.M.D. Hogeweij[1], J. Citrin[1], E. Westerhof[1], D. Peumans[2], M.R. de Baar[1,5]

[1]DIFFER-Dutch Institute for Fundamental Energy Research, PO Box 6336, 5600HH Eindhoven, The Netherlands
[2]Vrije Universiteit Brussel (VUB), Dept. of Fundamental Electricity and Instrumentation, Pleinlaan 2, 1050 Brussels, Belgium
[3]Eindhoven University of Technology, Dept. of Mechanical Engineering, Dynamics and control group, PO Box 513, 5600 MB Eindhoven, The Netherlands
[4]University of Twente, Dept. of Applied Mathematics, PO Box 217, 7500AE, Enschede, The Netherlands
[5]Eindhoven University of Technology, Dept. of Mechanical Engineering, Control Systems Technology group, PO Box 513, 5600 MB Eindhoven, The Netherlands

1 Introduction

Old and recent experiments show that there is a direct response to the heating power of transport observed in modulated ECH experiments both in tokamaks and stellarators [1, 2, 3]. This is most apparent for modulated experiments in the Large Helical Device (LHD) and in Wendelstein 7 advanced stellarator (W7-AS) (and suggested in W7-X [4]) and is called "hysteresis in flux". In this work we show that

1. Observations of hysteresis in flux (direct response to power) can be perfectly reproduced by a broadened deposition profile;
2. Non-local models can also explain the experimentally observed hysteresis in flux;
3. Power dependence/hysteresis in flux can be reproduced by linear models, i.e., no relationship to classic definitions of hysteresis (persistant memory) [5].

2 Perturbative experiment

The fundamental idea of perturbative experiments (see Fig. 1) is to have a sufficiently small (heating) perturbation such that the resulting (temperature) response can be considered linear [6]. This has been tested for the experiments where "hysteresis in flux" is observed and is generally the case if the experiment is well designed [6, 7, 8].

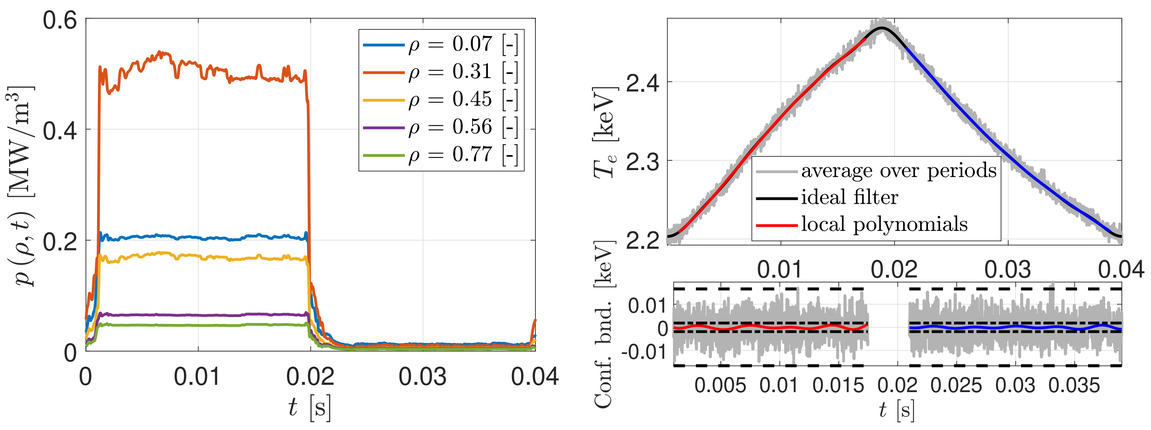

Fig. 1: Time evolution of electron heating and resulting electron temperature evolution at one radial location for one period (averaged) in the Large Helical Device (reproduced from [9])

3 Effect of broadened deposition profile on temperature evolution

The effect on the electron temperature of various deposition profiles is shown in Fig. 2.

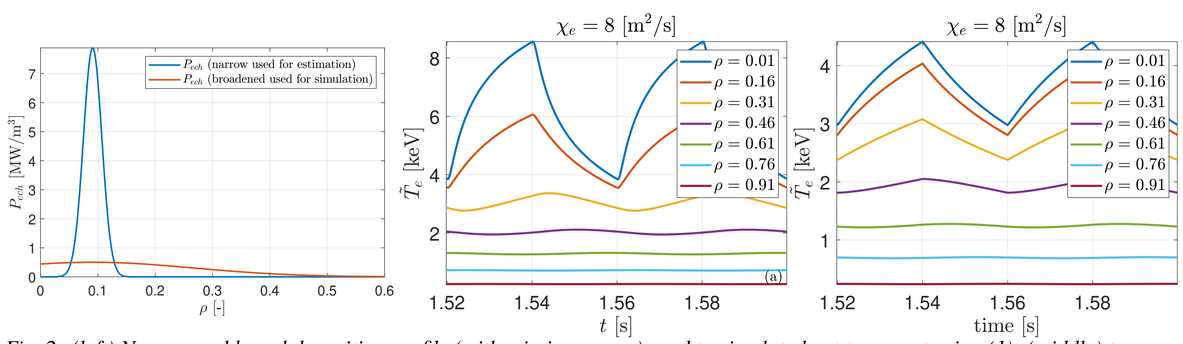

Fig. 2: (left) Narrow and broad deposition profile (with missing power) used to simulate heat transport using (1); (middle) temperature evolution: narrow deposition profile; and (right) temperature evolution: broad deposition profile

Note the similarity of the simulated temperature evolution shown in Fig. 2 (right) for a broadened deposition profile to that shown in Fig. 1 (right).

4 Hysteresis in flux

The measurements in Fig. 1 are used to calculate the heat flux, resulting in the "hysteresis in flux" figures [2, 10] and is claimed as proof of non-local transport:

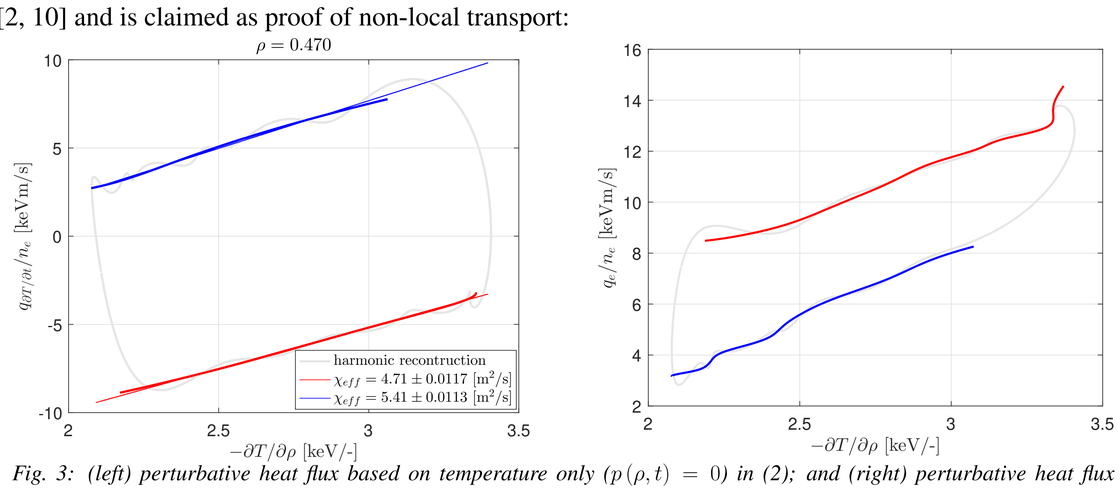

Fig. 3: (left) perturbative heat flux based on temperature only ($p(\rho,t) = 0$) in (2); and (right) perturbative heat flux including the heat source in (2). Reproduced from [9] same experiment as shown in Fig. 1.

In the case $q_e = -n_e\chi_e\partial T_e/\partial_\rho$ and if the deposition profile is perfectly known (no non-local transport), then we would expect the path to go up and down a straight line, i.e., the red and blue lines would coincide.

5 Error in deposition profile

To understand why an error in the deposition profile can (also) reproduce hysteresis in flux measurements, we analyze its calculation based on the heat equation [2]:

$$\frac{\partial}{\partial t}\left(n_e T_e(\rho,t)\right) = -\nabla_\rho q_e(\rho,t) + p(\rho,t) \tag{1}$$

with the electron temperature T_e, density n_e, heat flux q_e, heat source term $p(\rho,t)$ all as function of the dimensionless radius ρ. Hence, the heat flux can be calculated in cylindrical coordinates by [2, 8]

$$q_e(\rho,t) = \underbrace{\frac{1}{\rho}\int_0^\rho \rho\frac{\partial}{\partial t}\left(n_e T_e(\rho,t)\right)}_{q_{\partial T/\partial t}} \underbrace{-\frac{1}{\rho}\int_0^\rho \rho p(\rho,t)\,d\rho}_{q_P}. \tag{2}$$

We can reproduce Fig. 3 based on (linear) simulations of (2) by introducing an error on the deposition profile. Then (1) is simulated with a broader deposition profile and q_e is calculated using (2). For $p(\rho,t)$ a narrow deposition profile is used. This combination results in Fig. 4. and Fig. 5 for the source q_P.

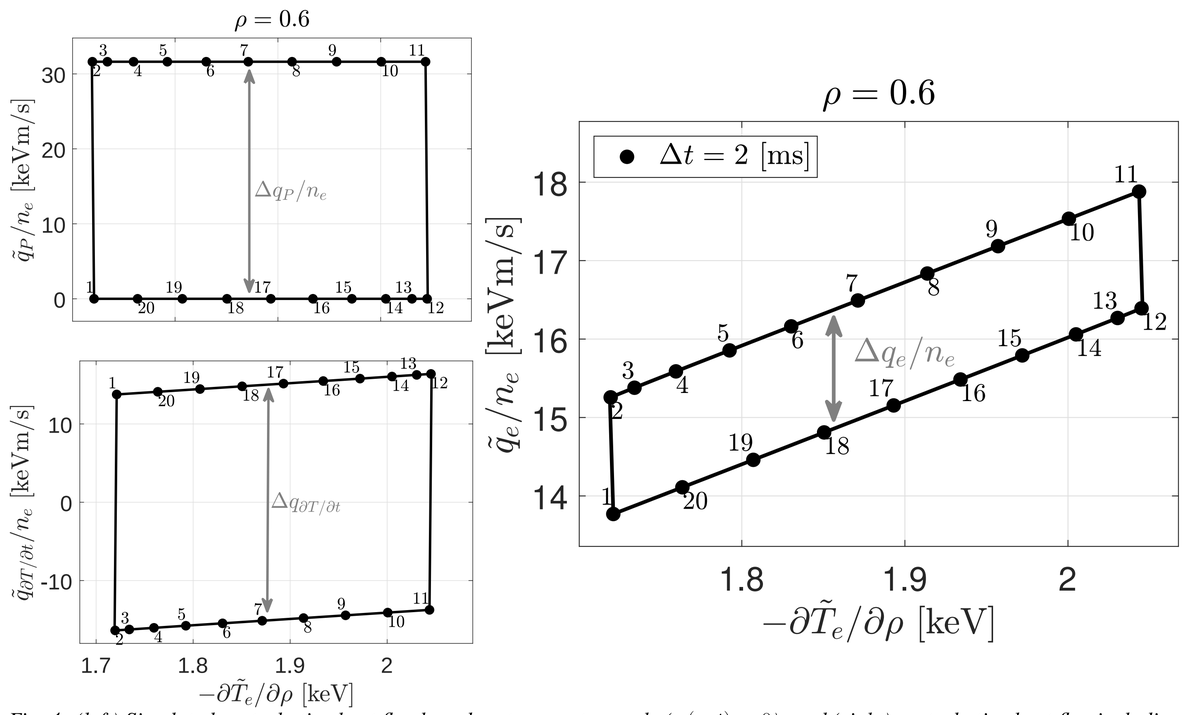

Fig. 4: (left) Simulated perturbative heat flux based on temperature only ($p(\rho,t) = 0$); and (right) perturbative heat flux including the heat source.

The difference between $q_{\partial T/\partial t}$ and q_P in (2) determines if, and how large, the gap is in $\tilde{q}_e/n_e$ (Fig. 4 and Fig. 3). Thereby showing that errors in the estimation deposition profiles can lead to apparent "hysteresis in flux". Note, that one can also prove that the linearization of classic non-local models [8, 10], e.g., $q_e = -n_e\chi_e(P)\nabla_\rho T_e$, can be rewritten as an apparent deposition profile [3]. Recent work also shows that when analyzing the EC heating deposition profile can be significantly broadened due to scattering of the EC-beam due to density fluctuations in the edge region [11, 12, 13, 14].

6 Discerning apparent deposition profiles from diffusion coefficients

The diffusion coefficients and the apparent deposition profile can be simultaneously determined (Fig. 7) [3, 9].

On the other hand, it is (mathematically) impossible to distinguish non-local transport from errors in the deposition profile estimate when analyzing linear perturbative experiments only. Hence, the next step is the analysis of diffusion coefficients and apparent deposition profiles over different equilibria.

7 Conclusion

Observed "hysteresis in flux" behavior is reproducible by linear models and can be fully explained by both old/new non-local models and/or errors in deposition profiles. Both models are mathematically equivalent.

[1] U. Stroth, L. Giannone et al., Plasma Phys. Control. Fusion 38, 4 1996.
[2] S. Inagaki, T. Tokuzawa, et al., Nucl. Fusion, 53, 113006, 2013.
[3] M. van Berkel, G. Vandersteen et al., Nucl. fusion, 58, pp. 106042, 2018.
[4] R. Wolf, C. Beidler, et al., 45th EPS Conference on Plasma Physics, I4.114, 2018.
[5] I. D. Mayergoyz, Mathematical models of hysteresis and their applications, 2003.
[6] N.J. Lopes Cardozo, Plasma Phys. Control. Fusion, 37, 799, 1995.
[7] M. van Berkel, G. Vandersteen et al., Nucl. fusion, 57, 126036, 2017.
[8] U. Stroth, B. Branas, Physica Scripta, 51, 655, 1995.
[9] M. van Berkel, T. Kobayashi, et al., Nucl. Fusion, 58, 096036, 2018.
[10] K. Itoh S.-I Itoh, et al., J. Phys. Soc. Jpn, 85, 014501, 2016
[11] J. Decker, Y. Peysson and S. Coda, EPJ Web of Conf. 32, 01016, 2012
[12] M. W. Brookman, M. E. Austin, et al., EPJ Web of Conf. 147, 03001, 2017
[13] A. Köhn, M.E. Austin, et al., EC20, 2019.
[14] O. Chellaï, S. Alberti, et al., Phys. Rev. Lett. 120, 105001, 2018

This work has been carried out within the framework of the EUROfusion Consortium and has received funding from the Euratom research and training programme 2014-2018 under grant agreement No 633053. The views and opinions expressed herein do not necessarily reflect those of the European Commission.